0031-3998/05/5802-0283
PEDIATRIC RESEARCH

Vol. 58, No. 2, 2005
Printed in U.S.A.

Pathologic and Immunohistochemical Findings in Hypothalamic and Mesencephalic Regions in the *Pah*^{enu2} Mouse Model for Phenylketonuria

JENNIFER E. EMBURY, ROGER R. REEP, AND PHILIP J. LAIPIS

Department of Biochemistry and Molecular Biology [J.E.E., P.J.L.], College of Medicine, and the Department of Physiological Sciences [R.R.R.], College of Veterinary Medicine, University of Florida, Gainesville, Florida 32610

ABSTRACT

The *Pah*^{enu2} mouse, created through ethylnitrosurea mutagenesis, is a model for phenylketonuria. These mice have elevated serum phenylalanine levels, hypopigmentation, and behavior and movement abnormalities, and female mice exhibit a maternal phenylketonuria syndrome. We evaluated the brains of adult and juvenile *Pah*^{enu2} mice for consistent, demonstrable lesions to elucidate various neuropathologic processes and to assess the efficacy of various treatment modalities such as AAV-mediated gene therapy. One aspect of the disease may involve the effect of hyperphenylalanemia on catecholamine function. High levels of phenylalanine inhibit enzymes that are important in the conversion of tyrosine and tryptophan to their respective neurotransmitter derivatives, including dopamine. Therefore, assessment of dopaminergic regions was of interest in this study. Histologic evaluation of juvenile and adult brains revealed an increased cellular density as early as 4 wk of age in the middle to posterior hypothalamus and substantia nigra. The infiltrating cells showed immunoreactivity for CD11b and had morphologic characteristics of macrophages. There was marked expression of inducible nitric oxide synthase in these dopaminergic regions that colocalized to CD11b-positive cells. The CD11b-positive cells and increased inducible nitric oxide synthase expression in these regions may function in a neuroregulatory manner to compensate for alterations in dopamine metabolism. (***Pediatr Res* 58: 283–287, 2005**)

Abbreviations

DA, dopamine
H&E, hematoxylin and eosin
iNOS, inducible nitric oxide synthase
MPTP, 1-methyl-4-phenyl-1,2,3,6-tetrahydropyridine
PHE, phenylalanine
PKU, phenylketonuria
SN, substantia nigra
SNpc, substantia nigra pars compacta
TH, tyrosine hydroxylase
TYR, tyrosine

The recessive metabolic disorder phenylketonuria (PKU) is among the most common human genetic defects, with an incidence of ~1 in 16,000 births in the United States. Several comprehensive reviews, which discuss both the biology and the genetics of PKU as well as other aspects of the disorder, are available (1,2). PKU results from an inability to convert phenylalanine (Phe) to tyrosine (Tyr), the first step in Phe catabolism. The resulting abnormal accumulation of Phe in infants with untreated PKU leads to a number of symptoms, the most important of which is significant disturbances in neonatal cognitive development with severe mental retardation. High levels of Phe are postulated to disrupt amino acid transport and metabolic pathways involving any of the aromatic amino acids, as well as protein synthesis, affecting both brain development and function. One likely mechanism for this abnormal development and function is that high Phe levels competitively inhibit movement of all of the large neutral amino acids across the blood-brain barrier. These amino acids all share a common transporter; thus, the result of high Phe levels is decreased uptake of the other large neutral amino acids and distortion of pool sizes. It is interesting that the large neutral amino acid carrier has a higher affinity for Phe than for other amino acids across many species; this increased affinity is more marked in humans than in rodents (3). High Phe levels may also specifically inhibit enzymes that are important in the conversion of Tyr and tryptophan to their respective neurotransmitter derivatives, particularly dopamine (DA) (4).

The *Pah*^{enu2} mouse is a suitable model to study PKU as it exhibits similar clinical characteristics as human patients that

Received July 29, 2004; accepted January 11, 2005.
Correspondence: Jennifer E. Embury, D.V.M., Department of Biochemistry and Molecular Biology, P.O. Box 100245, College of Medicine, University of Florida, Gainesville, FL 32610; e-mail: jembury@ufl.edu.
Supported in part by the National Institutes of Health (DK58327) and March of Dimes (6-FY02-155).

DOI: 10.1203/01.PDR.0000170000.78670.44

include hyperphenylalanemia, hypopigmentation (5,6), and cognitive defects. Cabib *et al.* (7) found these mice to have cognitive deficits that involve spatial and nonspatial recognition that is separate from motor impairment and not related to emotional reactivity to novel situations. They specified that the motor impairments in these mice include reduced locomotor activity and decreased rearing behavior. Puglisi-Allegra *et al.* (8) demonstrated significantly reduced DA content in the prefrontal cortex, nucleus accumbens, caudate putamen, and amygdala in these mice. In the prefrontal cortex, nucleus accumbens, and caudate putamen, there was also a marked reduction of DA release. Joseph and Dyer (9) showed that by placing the PKU mice on a low-Phe diet, DA and myelin basic protein were increased to near-normal levels in the striatum and frontal cortex, indicating a positive relationship between myelination and DA production.

Because dopaminergic systems seem to be affected in PKU, we chose to assess these regions in *Pah*^{enu2} mouse brains because detailed neuropathologic evaluation had not been performed to date. These brains were found to have increased numbers of activated microglia or macrophages along with increased inducible nitric oxide synthase (iNOS) immunoreactivity in the substantia nigra (SN) and hypothalamus, which occurred as early as 4 wk of age.

METHODS

Animal use and tissue collection. We have established a breeding colony of SPF *Pah*^{enu2} mice. The *Pah*^{enu2} mouse was created by ethylnitrosurea mutagenesis of male BTBR mice. The mutation is a T to C transition, changing Phe 263 to Ser, and incidentally creates a new Alw261 restriction fragment length polymorphism (10) in exon 7 of mouse chromosome 10. For genotyping offspring, a genomic fragment that contained exon 7 was amplified and digested with Alw26I to confirm the *Pah*^{enu2} mutation.

Adult and juvenile homozygous, heterozygous, and wild-type animals of both sexes were used. Juvenile age groups included 3, 8, and 10 wk; adult animals ranged from 6 mo to 1 y of age. A minimum of three animals were used to evaluate each sex, genotype, and age group for morphologic and immunohistochemical studies. Animals were deeply anesthetized with sodium pentobarbital (80 mg/kg, i.p.), exsanguinated, and perfused intracardially with 4% paraformaldehyde. This method is in accordance with the AVMA panel on euthanasia. This study was approved by the University of Florida Animal Care Services Department (IACUC), which is an AALAC-accredited facility.

After perfusion, the skull was opened and then fixed for 24 h in 4% paraformaldehyde. Brains were removed from the skull and transferred to 70% ethanol until processing and embedded in paraffin wax. The entire brain was serially sectioned (4-μm-thick sections), and every 10th section was stained with hematoxylin and eosin (H&E). Adjacent unstained sections were maintained for immunohistochemical studies.

Immunohistochemistry. Sections of brain tissue were immunostained with the following primary antibodies: CD11b and rat anti-mouse (Serotec, Raleigh, NC); anti-iNOS, rabbit polyclonal, and ABR (Golden CO); and mouse monoclonal anti-Tyr hydroxylase (Chemicon, Temecula, CA) using an ABC kit from Vector Laboratories (Burlingame, CA). Briefly, slides that were prepared as described above were deparaffinized and antigen exposure was achieved using the Trilogy antigen retrieval system (Cell Marque, Hot Springs, AR). Suppression of endogenous peroxidase activity was performed with 3% H_2O_2 for 5 min. Nonspecific binding was blocked with 3% normal serum for 30 min and application of streptavidin and biotin (Streptavidin/Biotin Blocking Kit; Vector). Tissues were incubated overnight at 4°C with appropriate primary antibody in 3% normal serum and 0.1% Triton-X at dilutions ranging from 1:50 to 1:100. An appropriate secondary biotinylated antibody (1:100–1:200) that contained 1% normal serum was applied, followed by incubation with avidin-biotin-peroxidase (Vector) conjugate and visualized with the appropriate Chromagen (Vector).

The fluorescent double-label protocol was carried out in a similar manner using Trilogy antigen retrieval. An initial blocking step with 10% donkey serum preceded application of primary iNOS antibody (1:50) for 1 h followed by fluorescein-conjugated donkey anti-rabbit (1:200; Molecular Probes, Eugene, OR) for 30 min. Sections then were incubated in 3% rabbit serum followed by a 1-h application of 1:50 rat anti-mouse CD11b primary antibody and rabbit anti-rat biotinylated secondary antibody 1:100 (Vector) and labeled with Texas Red Streptavidin (Vector) for 30 min. Negative controls for all studies were carried out under the same conditions using normal serum in place of primary antibody.

Measurement of hypothalamic periventricular cellularity. Sections that were stained with H&E from six groups (f−/−, m−/−, f+/−, m+/−, f+/+, m+/+; n = 6/group) of adult *Pah*^{enu2} mice were evaluated histologically by assessing entire brains of each animal, examining 4-μm sections at 40-μm intervals. Visual observations of increased numbers of cells surrounding the medial to posterior hypothalamic periventricular regions were confirmed using Zeiss-Axioplan morphometric microscope with MCID-M5 5.1 software. The sum of stained cellular nuclei in four fields (area of 1 field = 52772 μm^2) immediately surrounding both the right and the left, as well as ventral and dorsal aspects of the third ventricle, was determined in all six groups using morphometric grain-counting analysis. The area of measurement was restricted to the rostral aspect of the ventromedial hypothalamic nuclei and extended caudally to the dorsal and lateral arcuate nuclei and dopaminergic group A12. Exclusion parameters were set to identify the larger nuclei of the infiltrative cells, which had a dense homogeneous chromatin pattern and a nuclear diameter of 3–5 μm^2. The program was set to ignore the vesicular nuclei of neuronal cell bodies that had smaller nucleoli and chromatin particles that were <2–3 μm^2. Anatomic regions were identified using Paxinos and Franklin's mouse brain atlas (11). The cellular density of hypothalamic regions of each group were compared by ANOVA and t test. Data are presented as mean ± SEM unless otherwise noted. Probability values of $p < 0.05$ were considered significant.

Morphologic and immunohistochemical assessment of hypothalamic and mesencephalic regions. Juvenile mice that ranged in age from 3 to 10 wk were used for morphologic and immunohistochemical studies of hypothalamic and mesencephalic regions. H&E serial sections of the entire brain of each mouse were prepared and examined as described in "Methods." Increased numbers of cells were observed in hypothalamic and mesencephalic regions of juvenile PKU mice, similar to the findings in the adult animals. Within the mesencephalon, the infiltrate was especially notable within the pars reticulata and, to a lesser extent, the pars compacta. Selected sections from individual juvenile and adult mice were chosen for H&E and immunohistochemical studies. A minimum of three animals were evaluated for each sex, genotype, and age group for immunohistochemical analysis.

RESULTS

Periventricular cellularity in posterior hypothalamic nuclei is increased in homozygous* Pah^{enu2} *adult mice. We identified a region of increased cellularity surrounding the third ventricle in medial to posterior hypothalamic nuclei; this observation was quantified by Zeiss-Axioplan morphometric analysis (Fig. 1). This cellularity was significantly increased in both adult male and female homozygous recessive mice ($n = 6$; $p < 0.05$), compared with heterozygote and wild-type mice. It is interesting that female PKU mice ($n = 6$; $p < 0.05$) were significantly more affected than male PKU mice. The affected regions in both male and female PKU mice included the dorsomedio-ventromedial hypothalamic nuclei, central ventromedial hypothalamic nuclei, ventrolateroventromedial hypothalamic nuclei, dorsal and lateral arcuate nuclei, and dopaminergic group A12. The affected regions were observed to extend posteriorly to the dorsal and ventral premamillary nuclei. The increased cellular infiltrate within these regions was characterized by round to fusiform cells that were ~10–15 μm in diameter and had moderate amounts of eosinophilic cytoplasm. Nuclei were round with a deeply basophilic homogeneous chromatin pattern and inconspicuous nucleoli. The cellular infiltrate was most consistent with macrophage morphology. Within the described hypothalamic regions, the cellular infiltrate was approximately double the number of cells that were present in wild-type animals. The infiltrative cell population ob-

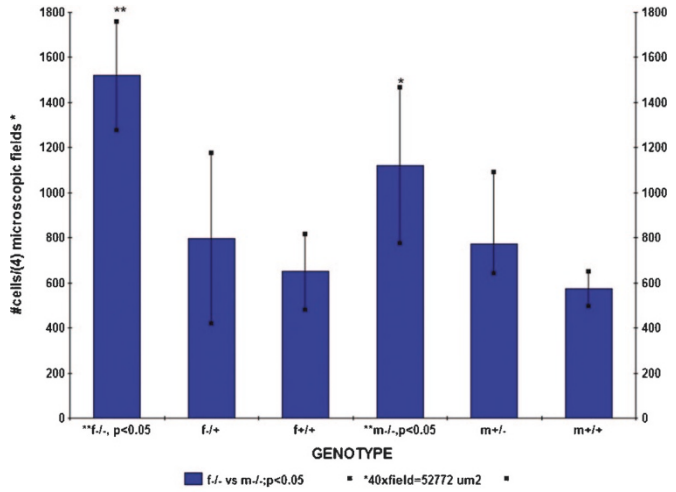

Figure 1. Periventricular cellularity in PKU mice. Morphometric analysis reveals increased hypothalamic periventricular cellularity in a region extending from the ventromedial hypothalamic nuclei to dorsal and lateral arcuate nuclei and dopaminergic group A12. The cellular infiltrate was significantly increased in male and female PKU mice compared with heterozygotes and wild-type mice. These mice ranged from 6 to 9 mo of age. Female PKU mice were significantly more affected than male PKU mice ($n = 6$; $p < 0.05$).

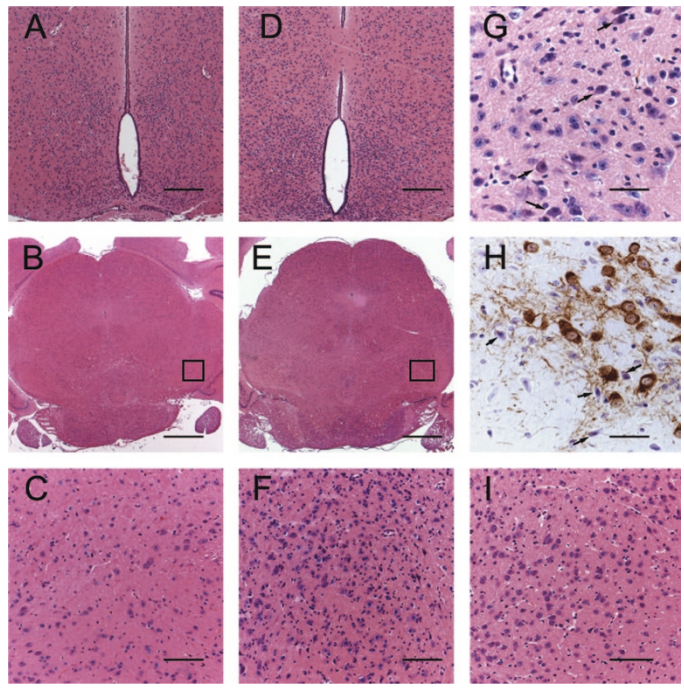

Figure 2. The normal morphology of dorsomedial and ventromedial hypothalamic nuclei in a 9-wk-old wild-type male mouse (*A*) is readily distinguished, when compared with the increased cellular infiltrate within the periventricular hypothalamic nuclei of an 8-wk-old homozygous recessive male mouse (*D*). The increased number of cells in this region is approximately doubled in the homozygous recessive mouse and obscures the normal periventricular morphology (*D*). The pars compacta and pars reticulata have a moderate to marked cellular infiltrate in PKU female mice at 8 wk (*E* and *F*) and occurs as early as 4 wk (*I*). The SN of a 9-wk-old wild-type female (*B* and *C*) is within normal limits. High-power magnification reveals numerous round cells (arrows, *G*) that are 8–10 μm in diameter with amphophilic cytoplasm, round nuclei, deeply basophilic homogeneous chromatin pattern, and inconspicuous nucleoli. These cells are pictured in the SN of 8-wk-old PKU mice. Infiltrative cells are present within the pars compacta of a male PKU mouse adjacent to DA neurons (TH; arrows, *H*). The infiltrative cells present in the pars compacta of PKU mice occasionally feature TH immunoreactive cytoplasmic granules. (*A* and *D*) H&E; bar = 100 μm. (*C* and *F*) H&E; bar = 50 μm. (*G*) H&E; bar = 25 μm. (*H*) TH immunoperoxidase method; bar = 25 μm.

scured the normal periventricular morphology, resulting in a diffuse cellular pattern (Fig. 2*A* and *D*). Similar changes were observed in juvenile 8-wk-old male and female PKU mice.

Morphologic evaluation of mesencephalic regions in adult and juvenile mice. Mesencephalic regions were assessed in adult and juvenile PKU mice and found to have a moderate to marked scattered infiltrate predominantly in the SN pars reticulata and ventral tegmental area (Fig. 2*E*) when compared with heterozygote and wild-type mice (Fig. 2*B*). The infiltrate occurred to a lesser degree in the SN pars compacta (SNpc). This cellular infiltrate was similar to that observed in the hypothalamic regions and occurred in juveniles as early as 4 wk of age (Fig. 2*I*). When viewing this region under low magnification (Fig. 2*B* and *E*), the distinctive, sharply delineated morphologic structure of the pars compacta and ventral tegmental area was moderately obscured in the homozygous recessive mouse. This was due to a mild scattered infiltrate in this region that resulted in loss of definitive distinction between the pars compacta and pars reticulata (Fig. 2*C* and *F*). The increased cellularity was predominantly evident within the pars reticulata but occurred in the pars compacta to a lesser degree. These infiltrative cells were round to slightly spindle-shaped, approximately 8–10 μm in diameter, and had moderate amounts of amphophilic cytoplasm (Fig. 2*G*). Nuclei were round and deeply basophilic with a condensed chromatin and inconspicuous nucleoli. There was occasional phagocytosis of adjacent neurons and glial cells. Tyr hydroxylase (TH) immunohistochemistry (Fig. 2*H*) demonstrated that this infiltrative cell population occurred near dopaminergic cell bodies as well as in the pars reticulata. Incidentally, increased cellular density was also observed in the medial and mediolateral medial mammillary nuclei in adult and juvenile homozygous mice. These mesencephalic changes were not readily detected in one male and two female PKU mice at 3 wk of age (unpublished observation).

Immunohistochemical studies. The infiltrative cells in dopaminergic regions of both male and female PKU mice were immunoreactive for the macrophage marker CD11b antigen and had morphologic features that were consistent with a macrophage cell type (Fig. 3*A* and *B*). The infiltrative cells that were present in the pars compacta of PKU mice occasionally featured intracytoplasmic granules that were immunoreactive for TH, which may be indicative of phagocytosis of adjacent DA neurons (Fig. 2*H*). Marked expression of iNOS was present in the SN (Fig. 3*C* and *D*) and hypothalamus (data not shown) of PKU mice. The marked iNOS expression in the mesencephalon was restricted to the SN/ventral tegmental region, resulting in a distinct pattern that was limited to these structures (Fig. 3*F*). Marked iNOS expression was not observed in nondopaminergic regions of PKU mice (Fig. 3*F*, inset) or the SN of wild-type mice (Fig. 3*E*). iNOS expression was associated with the infiltrative cell population as well as neuronal cell bodies in the pars compacta. The infiltrative cell

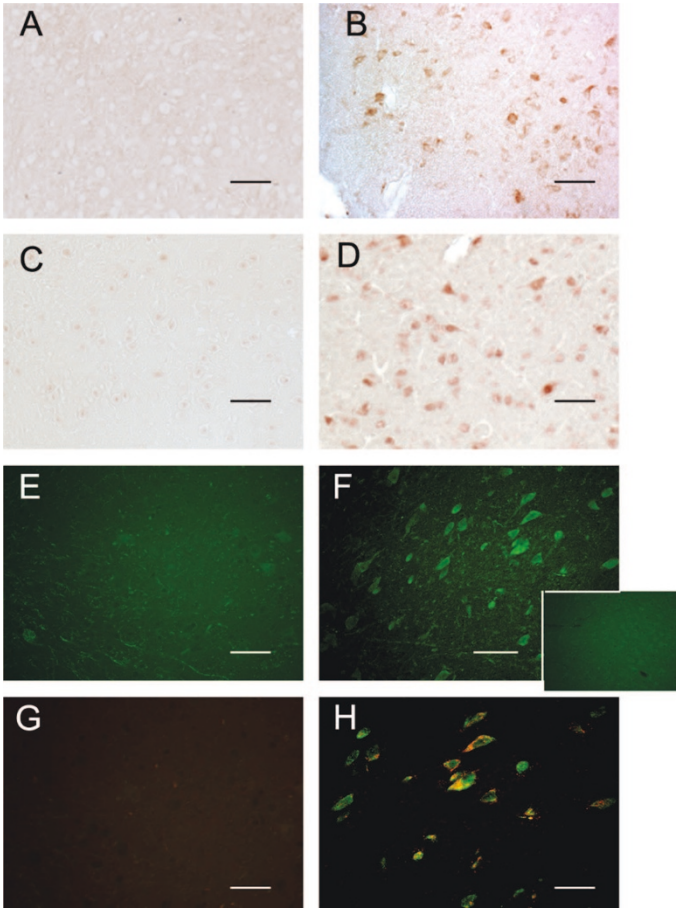

Figure 3. Comparison of wild-type mice (*A* and *C*) with homozygous recessive mice (*B*) shows immunoreactivity for CD11b antigen (*B*) and iNOS (*D*) in the SN of 8-wk-old PKU mice. CD11b (*A*) or iNOS (*C*) immunoreactivity was not observed in the SN of wild-type mice. Marked iNOS expression in the mesencephalon of PKU mice resulted in a distinct pattern that was limited to the SN and ventral tegmental regions (*F*). iNOS expression was not observed in nondopaminergic regions of PKU mice (*F*, inset) or the SN of wild-type mice (*E*). Co-localization of iNOS (fluorescein) and CD11b (rhodamine) in the SN of 8-wk-old PKU mice (*H*) is not observed in wild-type mice (*G*). (*A* and *B*) CD11b immunoperoxidase method. (*C* and *D*) iNOS immunoperoxidase method; bar = 50 μm. (*E*, *F* and *F inset*) Immunofluorescence with directly conjugated fluorescein antibody (iNOS); bar = 25 μm. (*G* and *H*) Double-label immunofluorescence with directly conjugated fluorescein antibody (iNOS) and Texas Red Streptavidin (CD11b). Bar = 25 μm.

population within the SN of PKU mice demonstrated co-localization of CD11b antigen and marked iNOS expression (Fig. 3*H*) when compared with wild-type mice (Fig. 3*G*). Astrocytic cells were unremarkable with glial fibrillary acidic protein immunohistochemistry in the affected SN or hypothalamic regions of PKU mice (data not shown).

DISCUSSION

The posterior division of the arcuate nucleus, medial mammillary nuclei, ventral and dorsal premamillary nuclei, and the A12 nucleus are regions that are rich in dopaminergic cells and dopaminergic receptor distribution. Dopaminergic areas are more widely distributed in the midbrain, and these regions are involved in a host of autonomic functions and regulation of DA function. Histologic evaluation of entire *Pah*^{enu2} juvenile and adult brains revealed an increased cellular density in the middle to posterior hypothalamus and mesencephalon, notably in the SN pars reticulata and pars compacta. Increased cellular density was incidentally observed in medial and mediolateral medial mammillary nuclei. The infiltrative cell population was unremarkable in 3-wk-old mice but dramatically increased in 4-wk-old homozygous mice.

The infiltrative cells in dopaminergic regions of these PKU mice had morphologic characteristics consistent with infiltrating macrophages and showed immunoreactivity for CD11b and iNOS. Astrocytic cells were unremarkable in the SN or hypothalamus of these mice, and these results concur with a study by Dyer *et al.* (12), which stated that astrocytes did not seem to be the source of the gliosis in PKU mice that they studied. In general, CD11b immunostaining can identify both resting and activated macrophages. Resting microglia constitutively express the complement type 3 receptor (CR3; CD11b/CD18 complex), which is further up-regulated upon activation (13). The infiltrative cells in these PKU mice express immunoreactivity for CD11b; however, these cells may represent a mixed population, developmentally ranging from microglial to macrophage cell types, and further studies are under way to characterize the population.

There was increased iNOS expression by the infiltrative cells in the present study within the mesencephalic and hypothalamic regions of PKU mice. In a review by West *et al.* (14), it was established that NO can facilitate DA transmission in nerve terminals and also has neuroprotective effects in oxidative damage *via* quenching of superoxide anions. The most consistent effect observed within these studies pertaining to the role of exogenous NO or NO generators is facilitation of DA release. However, there is a report showing that NO gas and the NO donor +/− S-nitroso-N-acetylpenicillamine decreased striatal release, whereas the non–NO-containing carrier molecule penicillamine elevates DA efflux (15). It is interesting that these discrepancies may be related to the redox state of the tissue sampled in the particular biologic preparation (16,17).

Ercal *et al.* (18) showed that malondialdehyde, a marker of lipid peroxidation, was significantly higher in the brains and red blood cells of PKU mice. Both catalase and glucose-6-phosphate dehydrogenase were significantly increased in the red blood cells of PKU mice, also indicating oxidative stress. Colome *et al.* (19) observed in patients with PKU similar findings that showed increased malondialdehyde along with other biochemical markers of oxidative stress and concluded that plasma lipid peroxidation is increased in these patients.

Hagen *et al.* (20) demonstrated in an experimentally induced rat model of hyperphenylalanemia that excessive Phe stimulates oxidative stress in the brain. They concluded that increased Phe showed increased free-radical production and compromises the total antioxidant capacity of the nervous tissue.

These studies show that oxidative stress in patients and animals with PKU is likely a direct effect of hyperphenylalanemia and could be due to many causes that may include TH action on excess Phe, resulting in the production of dihydroxyphenylalanines. Oxidation of these catecholamines can result in the production of superoxide and hydrogen peroxide (21). The infiltrative cells may be a response to oxidative stress. The

increased iNOS expression demonstrated in the mice in the present study may serve as a neuroprotective role in quenching superoxide anions, as West *et al.* (14) suggested.

Conversely, it is also possible that the NO behaves in a deleterious manner. The deleterious action of microglial iNOS-derived NO was illustrated by Libertore *et al.* (22). They reported a robust gliosis in the SNpc associated with significant up-regulation of iNOS, and these changes preceded or paralleled 1-methyl-4-phenyl-1,2,3,6-tetrahydropyridine (MPTP)-induced dopaminergic neurodegeneration. They contended that the microglial response to MPTP arises early enough in the neurodegenerative process to contribute to the demise of SNpc dopaminergic neurons. Similar histologic and immunohistochemical findings were observed in the PKU mice in the present study. It is possible that increased NO production in the PKU mouse model may also contribute to neuronal degeneration.

It was suggested that NO acts to decrease DA release under conditions in which oxygen radical production is accelerated and antioxidants are depleted (15). Puglisi-Allegra *et al.* (8) established that a reduction in dopaminergic content and release occurred in the prefrontal cortex, nucleus accumbens, and caudate putamen. It is feasible that increased NO production in dopaminergic regions (nigrostriatal structures) further contributes to decreased striatal release, accounting for the observations of Puglisi-Allegra *et al*.

In one previous study, Kornguth *et al.* (23) examined Phe hydroxylase–deficient mice and found no evidence of demyelination or other abnormalities by magnetic resonance imaging or histologic evaluation of the cerebellum, hippocampus, occipital cortices, and parietal/frontal cortices when compared with normal littermates. These results concur with our observations that there were no detectable histologic changes in these specific regions, although we did identify morphologic and immunohistochemical changes in the hypothalamus and mesencephalon. In addition, Joseph and Dyer (9) reported that when they used Luxol fast blue, a myelin-specific stain, there clearly was an increase in the amount of myelin in subcortical white matter, corpus callosum, and striatum of treated PKU mice compared with respective structures in untreated PKU mouse brain.

CONCLUSION

In conclusion, infiltrative CD11b macrophage-type cells observed within dopaminergic regions of PKU mice demonstrate marked iNOS expression in this study. It may be interesting to compare the pathologic processes of PKU with Parkinson's disease. A common feature of both PKU and Parkinson's disease is the reduction of normal DA concentrations in the brain. Parkinson's disease is characterized by a reduction in striatal DA content caused by the loss of dopaminergic neurons in the SNpc and of their projecting nerve fibers in the striatum (24). Clinically, Parkinson's disease is a disturbance in motor functions characterized by resting tremor, rigidity, stooped posture, gait disturbance, and slowing or hesitancy of voluntary movements (25). Similarly, the *Pah*^{enu2} mouse model has motor disturbances (7), and both disease models feature infiltrative CD11b cells with iNOS up-regulation in the SN. It may be useful to compare pathologic mechanisms in both of these models to provide insight on NO regulation of dopaminergic function. Increased NO may function as a neuroprotective or neuroregulatory role or may simply be a response to oxidative damage caused by hyperphenylalanemia.

Acknowledgments. We thank Dr. Matthew P. Galloway for insightful comments on the manuscript as well as inspiration and mentoring (J.E.E.). Special thanks to Dr. F. Gilles for guidance and support. We also thank Dr. Ron Mandel for helpful comments during manuscript preparation.

REFERENCES

1. Scriver CR, Kaufman S 2001 Hyperphenylalaninemia: phenylalanine hydroxylase deficiency. In: Scriver CR, Beaudet AL, Sly WS, Valle D (eds) The Metabolic and Molecular Bases of Inherited Disease, 8th Ed. McGraw-Hill, New York, pp 1665–1725
2. Blau N, Thony B, Cotton RGH, Hyland K 2001 Disorders of tetrahydrobiopterin and related biogenic amines. In: Scriver CR, Beaudet AL, Sly WS, Valle D (eds) The Metabolic and Molecular Bases of Inherited Disease, 8th Ed. McGraw-Hill, New York, pp 1726–1776
3. Pardridge WM 1998 Blood-brain barrier carrier-mediated transport and brain metabolism of amino acids. Neurochem Res 23:635–644
4. Kaufman S 1999 A model of human phenylalanine metabolism in normal subjects and phenylketonuric patients. Proc Natl Acad Sci USA 96:3160–3164
5. McDonald JD, Bode VC, Dove WF, Shedlovsky A 1990 Pah^{bph-5}: a mouse mutant deficient in phenylalanine hydroxylase. Proc Natl Acad Sci USA 87:1965–1967
6. Shedlovsky A, McDonald JD, Symula D, Dove WF 1993 Mouse models of human phenylketonuria. Genetics 134:1205–1210
7. Cabib S, Pascucci T, Ventura R, Romano V, Puglisi-Allegra S 2003 The behavioral profile of severe mental retardation in a genetic mouse model of phenylketonuria. Behav Genet 33:301–310
8. Puglisi-Allegra S, Cabib S, Pascucci T, Ventura R, Cali F, Romano V 2000 Dramatic brain aminergic deficit in a genetic mouse model of phenylketonuria. Neuroreport 11:1361–1364
9. Joseph B, Dyer CA 2003 Relationship between myelin production and dopamine synthesis in the PKU mouse brain. J Neurochem 86:615–626
10. McDonald JD, Charlton CK 1997 Characterization of mutations at the mouse phenylalanine hydroxylase locus. Genomics 39:402–405
11. Paxinos G, Franklin KB 1997 The Mouse Brain in Stereotaxic Coordinates. Academic Press, London
12. Dyer CA, Kendler A, Philibotte T, Gardiner P, Cruz J, Levy HL 1996 Evidence for central nervous system glial cell plasticity in phenylketonuria. J Neuropathol Exp Neurol 55:795–814
13. Streit WJ 2002 Microglia as neuroprotective, immunocompetent cells of the CNS. Glia 40:133–139
14. West AR, Galloway MP, Grace A 2002 Regulation of striatal dopamine neurotransmission by nitric oxide: effector pathways and signaling mechanisms. Synapse 44:227–245
15. Guevara-Guzman R, Emson PC, Kendrick KM 1994 Modulation of in vivo striatal transmitter release by nitric oxide and cyclic-GMP. J Neurochem 62:807–810
16. Buyukuysal L 1997 Effect of nitric oxide donors on endogenous dopamine release from striatal slices. I. Requirement of antioxidants in the medium. Fundam Clin Pharmacol 11:519–527
17. Trabace L, Kendrick KM 2000 Nitric oxide can differentially modulate striatal neurotransmitter concentrations via soluble guanylate cyclase and peroxynitrite formation. J Neurochem 75:1664–1674
18. Ercal N, Aykin-Burns N, Gurer-Orhan H, McDonald JD 2002 Oxidative stress in a phenylketonuria animal model. Free Radic Biol Med 32:906–911
19. Colomé C, Artuch R, Vilaseca MA, Sierra C, Brandi N, Lambruschini N, Cambra FJ, Campistol J 2003 Lipophilic antioxidants in patients with phenylketonuria. Am J Clin Nutr 77:185–188
20. Kienzle Hagen ME, Pederzolli CD, Sgaravatti AM, Bridi R, Wajner M, Wannmacher C, Wyse AT, Dutra-Filho CS 2002 Experimental hyperphenylalaninemia provokes oxidative stress in rat brain. Biochim Biophys Acta 1586:344–352
21. Halliwell B, Gutteridge J1989 Free Radicals in Biology and Medicine. Clarendon Press, Oxford
22. Liberatore GT, Jackson-Lewis V, Vukosavic S, Mandir AS, Vila M, McAuliffe WG, Dawson VL, Dawson TM, Przedboski S 1999 Inducible nitric oxide synthase stimulates dopaminergic neurodegeneration in the MPTP model of Parkinson's disease. Nat Med 5:1403–1409
23. Kornguth S, Anderson M, Markley JL, Shedlovsky A 1994 Near-microscopic magnetic resonance imaging of the brains of phenylalanine hydroxylase deficient mice, normal littermates, and of normal BALB/c mice at 9.4 Tesla. Neuroimage 1:220–229
24. Pakkenberg B, Moller A, Gundersen HJ, Mouritzen A, Pakkenberg H 1991 The absolute number of nerve cells in substantia nigra in normal subjects and in patients with Parkinson's disease estimated with an unbiased stereological method. J Neurol Neurosurg Psychiatry 54:30–33
25. Kumar V, Cotran R, Robbins SL 2003 Robbins Basic Pathology, 7th Ed. WB Saunders, Philadelphia, p 844